Histol Histopathol (2010) 25: 485-493

http://www.hh.um.es

Histology and Histopathology

Cellular and Molecular Biology

Etoposide induces G2/M arrest and apoptosis in neural progenitor cells via DNA damage and an ATM/p53-related pathway

C. Nam, K. Doi and H. Nakayama

Department of Veterinary Pathology, Graduate School of Agricultural and Life Sciences, The University of Tokyo, Tokyo, Japan

Summary. Etoposide (VP-16), an anti-tumor agent, is a topoisomerase II inhibitor that causes DNA damage. In our previous studies, it was shown that VP-16 induces S-phase accumulation and G2/M arrest, eventually resulting in apoptosis, through p53-related pathway in the mouse fetal brain. We injected 4 mg/kg of VP-16 into pregnant mice on day 12 of gestation, and the fetuses were investigated for the cell cycle checkpoint and mechanism of apoptosis. The transition of the neural progenitor cells in the fetuses was delayed as compared to that in the control, and most of the apoptotic cells were BrdU positive. VP-16-induced S-phase accumulation was brought about by the acceleration of G1/S transition rather than by the inhibition of S-phase progression. Phosphorylation of ataxia telangiectasia-mutated kinase (ATM) at Ser1981 and γH2AX after VP-16 treatment showed DNA damage. p53 was phosphorylated at Ser15 and 20 and increased after activation of the ATM kinase pathway. Cdc25A degradation might induce the inhibition of S-phase progression. It is supposed that an increase in cyclin A might accelerate G1/S progression. It is also indicated that VP-16-induced G2/M arrest is caused by p21, which inactivates cyclin B-Cdc2 complex and eventually prevents mitotic entry. In p53-deficient fetal brains, G2/M and apoptosis were almost abrogated, although S-phase accumulation still occurred. It is suggested that VP-16 induced p53-independent S-phase accumulation, and p53-dependent G2/M arrest and apoptosis of the neural progenitor cells in fetal mouse brain.

Offprint requests to: Dr. Chunja Nam, Department of Veterinary Pathology, Graduate School of Agricultural and Life Sciences, The University of Tokyo, Tokyo 113-8657, Japan. e-mail: vet0215@yahoo.co.kr

Key words: Etoposide, DNA damage, Cell cycle checkpoint, Apoptosis, Neural progenitors

Introduction

VP-16, a topoisomerase II inhibitor, is widely used as a chemotherapeutic agent for small cell lung cancer, testicular cancers, and lymphomas (Sieber et al., 1978; Robinson and Oscheroff, 1991; Chen and Liu, 1994; Hande, 1998). VP-16 is also known to be a teratogen, and brings about skeletal malformations and the central nervous system (CNS) anomalies in mice and rats when administered during the early gestational stages (Sieber et al., 1978). VP-16 interferes with topoisomerase II activity and causes DNA double-strand breaks (DSBs) through the formation of a DNA-drug-enzyme cleavage complex (Gantchev and Hunting, 1997). VP-16 has been shown to immediately induce cell cycle arrest and apoptosis in the CNS of mouse fetuses when administered to pregnant mice on gestation day 12 (GD12) (Nam et al., 2006a,b).

During the early stages of neural tube development, undifferentiated neural stem cells proliferate by symmetric division. Their nuclear positions differ at different stages of the cell cycle. DNA synthesis (S) occurs when the nuclei are at the outer part of the neural tube. In the G2/M phase, the cells undergo mitosis and produce 2 daughter cells on the surface of the ventricle (Fujita, 2003). During neurogenesis, asymmetric divisions generate 2 daughter cells: one reenters the cell cycle (G1 to S) and the other differentiates into young neurons (neuroblasts: G0) and migrates from ventricular zone (VZ) to the marginal zone (MZ), where postmitotic neurons accumulate (Qian et al., 2000; Yoshigawa, 2000).

In embryonic day (E) 12 to E13 mice, approximately 70% of the cells in the fetal telencephalons are neural progenitor cells (D'Sa-Eipper et al., 2001); hence, it was considered that the cells were analyzed reflected the cell cycle distribution of neural progenitor cells. Most of the neural progenitor cells are known to be localized in the VZ rather than the subventricular zone (SVZ), and the neural progenitor cells proliferate very actively in the VZ at E12 and E13 because the SVZ is not yet remarkable (D'Sa-Eipper et al., 2001).

DNA damage agents like irradiation induce DSBs as well as cell cycle arrest and apoptosis via ATM-checkpoint kinase 2 (Chk2) responses (DiTullio et al., 2002; Ha et al., 2003). The p53 tumor suppressor protein is activated by DNA damage and other cellular stresses, which is followed by the induction of cell cycle arrest, DNA repair and apoptosis (Ko and Prives, 1996; Levine, 1997; Stewart and Pietenpol, 2001). In response to DNA damage agents, the neural progenitor cells in fetal mice has been shown to undergo apoptosis via a p53-dependent pathway (Katayama et al., 2005; Ueno et al., 2006).

In the present study, we investigated VP-16-induced DNA damage, cell cycle alternation, and apoptosis and their mechanisms in fetal mouse telencephalons by flow cytometry, immunohistochemistry and Western blot analysis after VP-16 administration to pregnant mice on GD 12. We also examined the histological changes, TUNEL staining and cell cycle analysis in the neural progenitor cells after VP-16 treatment in p53-knockout mice in order to investigate the role of p53 in VP-16-induced cell cycle arrest and apoptosis. We verified that VP-16 induces ATM activation, DNA damage, the p53-independent or p53-dependent pathway of neural progenitor cell cycle arrest and apoptosis.

Materials and methods

Chemicals

VP-16 and 5-bromo-2´-deoxyuridine (BrdU) were purchased from Sigma (St. Louis, MO). VP-16 was dissolved in 1% dimethyl sulphoxide (DMSO; Sigma) solution in physiological saline.

Animals

Eight-week-old pregnant ICR (Crj:CD-1) mice were purchased from Charles River Japan Co.(Yokohama, Japan), p53+/- mice (C5BL/6N-TgH(p53)) were provided by RIKEN BioResource Center (Tsukuba, Japan). Heterozygous mice were back-crossed to wild-type mice (heterozygote x C57BL/6CrSlc) to maintain and propagate the colony. Heterozygous mice were crossed to generate wild-type, heterozygous, and homozygous gene-disrupted mice. Genotyping was conducted by polymerase chain reaction (PCR) analysis of tail DNA extracts. The mice were maintained in an isolator cage (Niki Shoji Co., Tokyo) under controlled conditions (23±2°C with 55±5% humidity and a 14-hr light / 10-hr dark cycle); they were fed commercial pellets (MF; Oriental Yeast Co. Ltd., Tokyo) and provided with tap water *ad libitum*. All procedures were approved by the Animal Use and Care Committee of the Graduate School of Agricultural and Life Sciences, the University of Tokyo.

Genotype analysis of the p53-knockout mice (Tsukada et al., 1993)

Genomic DNA was extracted from the tail of fetuses or 4-week-old mice by using the DirectPCR Lysis Reagent (Viagen Biotech, Inc., CA, USA) by the proteinase K method. PCR amplifications were performed by using the LA Taq kit with GC buffer 1 (Takara, Japan). After an initial denaturation at 94°C for 7 min, amplification was performed using a Takara PCR Thermal cycler SP (Takara) (Table 1) under the following conditions: 30 sec of denaturation at 94°C, 30 sec of annealing at 57°C and 3 min of extension at 72°C. The primers used were a mixture of (1) LCB614 in intron 1, i.e., 5'-GTTATGCATCCATACAGTACA, and (2) LCB651 in exon 3, i.e., 5'-CAGGATATC TTCTGGAGGAAG. The PCR products were electrophoretically separated on 2% agarose S (Nippon Gene) in TBE buffer. The gels were stained with ethidium bromide (Gibco), and the fluorescent bands were visualized using a UV-CCD video system (EpiLightUVFA1100; AISIN COSMOS, Tokyo, Japan).

Treatment of the ICR mice

Eight-week-old pregnant mice were injected with 4 mg/kg of VP-16 intraperitoneally (ip) on GD 12. For the control, pregnant mice were injected with 1% DMSO solution ip on GD 12. The dam mice were sacrificed by exsanguination under ether anesthesia at 1, 2, 4, 8, 12, 24 and 48 hours after treatment (HAT). The collected fetuses were subjected to histopathological examination, cell cycle analysis and Western blot analysis.

Treatment of the p53-knockout mice

Pregnant mice were administered 4 mg/kg of VP-16 ip on GD 12. For the control, pregnant mice were injected with 1% DMSO solution ip on GD 12. The dam mice were euthanized at 4 and 12 HAT. The collected fetuses were subjected to histological examination, TUNEL staining and cell cycle analysis. The fetuses were fixed in 10% neutral-buffered formalin for histopathological examination and TUNEL staining.

Histological examination

The fetuses obtained from the dams as scheduled were fixed in 10% neutral-buffered formalin and

embedded in paraffin. Further, 4-μm paraffin sections were stained with hematoxylin and eosin (HE) for histopathological examination.

Cell cycle analysis

For cell cycle analysis, the telencephalons of 3 fetuses from each dam were obtained in Hanker's balanced salt solution. Cells from the telencephalons were washed in PBS and resuspended in 1 ml of PBS at a density of $1x10^6$ cells/ml. Ice-cold ethanol (2.7 ml) was added to it to yield a final ethanol concentration of 70%. After centrifugation, the cells were resuspended in 1 ml of PBS and incubated with 10 μl of RNAse at 37°C for 40 min. Ten microliters of propidium iodide (5 mg/ml) were then added. Forward scatter (FSC) and side scatter (SSC) analysis was performed to assess the changes in cell morphology and fluorescent lamp-2 height (FL-2H; red fluorescence) analysis was performed using a FACSCalibur Flow Cytometer (Becton-Dickinson, Franklin Lakes, NJ) to detect changes in the cellular DNA content and DNA fragmentation. Using the Cell Quest program (Becton-Dickinson), doublets and debris were discarded, and the percentages of cells in various phases of the cell cycle were calculated.

Cell cycle analysis of the BrdU-positive cells

BrdU incorporation assays were performed to investigate the transition of BrdU-incorporated cells in the cell cycle and to analyze the DNA-replicating cells after VP-16 administration by cell cycle analysis.

First, pregnant mice were simultaneously treated with 4 mg/kg of VP-16 and 20 mg/kg of BrdU ip on GD12. For the control, pregnant mice were injected with 1% DMSO solution and 20 mg/kg of BrdU ip on GD12. The fetal telencephalons of the 3 fetuses from each dam were obtained and subjected to cell cycle analysis at 1, 2, 4, 8, 12, 24, and 48 HAT.

Secondly, a BrdU incorporation assay was performed on the mouse fetuses collected at 4 HAT. Pregnant dam mice were injected ip with 20 mg/kg of BrdU exactly 1 hr before autopsy.

For the assessment of cell cycle kinetics, the cells were fixed in 70% ethanol, washed with PBS and resuspended in 0.5% Triton X-100 in 2 N HCl for 30 min at room temperature (RT). Following neutralization with 0.1 M $Na_2B_4O_7$, they were pelleted and washed with PBS. The cells were then stained with FITC-conjugated mouse anti- BrdU antibody (BD PharMingen) for 30 min in the dark at RT. They were then washed with 0.5% Tween 20 and 1% BSA in PBS, incubated with 2 μl of propidium iodide for 30 min on ice, and analyzed using the FACScalibur machine. Using the Cell Quest program (Becton-Dickinson), doublets and debris were discarded, and the percentages of cells in various phases of the cell cycle were calculated.

TUNEL method

DNA fragmentation was examined in the paraffin sections by a modified TUNEL (Terminal deoxynucleotidyl Transferase Biotin-dUTP Nick End Labeling) method, which has been widely used for the detection of apoptotic cells. A commercial apoptosis detection kit (ApopTag® Peroxidase In situ Apoptosis Detection Kit; Chemicon, CA) was used in the present study.

Immunohistochemistry

The formalin-fixed tissues were embedded in paraffin. The deparaffinized sections were immersed in a 10 mM citrate buffer (pH 6.0) and autoclaved at 120°C for 15 min. The endogenous peroxidase activity was quenched by immersing the sections in 0.3% H_2O_2 in methanol for 30 min. The sections were incubated in 8% skimmed milk at 37°C for 1 hr to reduce non specific reactions. Overnight incubation at 4°C with the primary antibody against γH2AX (Cell signaling) or cleaved caspase-3 (Cell signaling Technology) was then performed. The sections were further incubated with biotinylated secondary antibody (1:400; Kirkegaard and Perry) and then with streptavidin (1:300; Dako) for 1 hr at RT. The positive reactions were visualized by the peroxidase-diaminobenzidine method and then counterstained with methyl green.

Western blot analysis

The telencephalons were dissected from the fetuses pooled and lysed in a buffer containing 10 mM Tris–HCl (pH 8.0), 150 mM NaCl, 1% NP-40, 1 mM EDTA, 2 mM Na_3VO_4, 10 mM NaF, and x1 EDTA-free protease inhibitor cocktail solution (Roche, Penzberg, Germany). The protein concentration of the lysate was assessed by using Lowry's protein assay kit (Bio-Rad, Hercules, CA). Samples containing equal amounts of protein were electrophoresed on SDS polyacrylamide gels and transferred onto PVDF membranes (Bio-Rad). The membranes were blocked in TBS containing 0.1% Tween-20 and 5% skimmed milk before the addition of antibodies.

The primary antibodies used included anti-phospho-ATM-Ser1981 (Cell Signaling), anti-γH2AX (Cell Signaling), anti-phospho-c-Abl-Tyr245 (Cell Signaling), anti-p53 (Santa Cruz), anti-p21 (PharMingen), anti-cyclin A (Santa Cruz Biotechnology, Santa Cruz, CA), anti-cyclin B1 (Santa Cruz), anti-Chk2 (Cell Signaling), anti-phospho-p53-Ser15 (Cell Signaling), anti-phospho-p53-Ser20 (Santa Cruz), anti-Cdc2 (Cell Signaling), anti-phospho-Cdc2 (Cell Signaling), anti-Cdc25A (Santa Cruz), anti-puma (Sigma) and anti-ß-actin (Cell Signaling). Horseradish peroxidase-conjugated secondary anti-mouse or anti-rabbit IgG antibodies (Amersham) were used at a dilution of 1:10000.

Enhanced chemiluminescence kit (ECL+; GE HealthCare, UK) was used for signal detection and a CCD-camera (Bio-Rad) was used for detection and capture of a digital image.

Results

In our previous studies, we showed that VP-16 induced S-phase accumulation, G2/M arrest and apoptosis in fetal mouse brain (Nam et al., 2006b). The cell cycle fractions at 1 and 2 HAT after VP-16-injection were not significantly different from those of the control. The S and G2/M fractions increased significantly at 4 and 8 HAT as a result of VP-16 treatment. Furthermore, the sub-G1 fraction (apoptotic cells) of the VP-16-exposed fetuses began to increase significantly at 4 HAT, peaked at 12 HAT, decreased gradually at 24 HAT and then returned to the control level at 48 HAT.

The sequential changes in the number of BrdU-positive cells in the fetal brains are shown in Fig. 1. At 4 HAT, BrdU-incorporation in the fetal telencephalons was not significantly different as indicated. In addition, there were many cells containing DNA identical to that of the S-phase cells, and most of the S-phase cells had incorporated BrdU at 4 HAT. S-phase accumulation was brought about by the acceleration of G1/S-transition rather than by the inhibition of S-phase progression or DNA replication.

To confirm that the cells shifted from accumulation in the S and G2/M phases and either entered G0/G1 or became apoptotic, we injected BrdU (20 mg/kg) with a vehicle or VP16 at the same time and used flow cytometry to investigate the cell cycle transition of VP-16-exposed neural progenitor cells. VP-16 and BrdU both get incorporated into DNA during the S phase of the cell cycle. In the control group, BrdU was first incorporated into the S-phase cells at 1 and 2 HAT after treatment (Fig. 2). At 4 HAT, the BrdU-incorporated cells had transitioned from the S to G2/M phase, and some had entered the G0/G1 phase. At 8 HAT, most of the BrdU-positive cells had almost exited the S phase and were mainly in G0/G1, and some cells were still in G/2M. At 8 HAT, some BrdU-positive cells had started to re-enter the S phase, and most of them had returned to the S phase at 12 HAT. When VP-16 was injected with BrdU, BrdU also was first incorporated into the S phase cells at 1 and 2 HAT. At 4 HAT, more VP-16-treated cells than control cells were still in S and G2 phases. Many of these cells were likely in the G2 phase because the number of mitotic figures decreased at 4 HAT (Nam et al., 2006a). Furthermore, most of the BrdU-positive cells started to undergo apoptosis, as demonstrated by the increase in the sub-G1 area at 4 HAT. At 8 HAT, many of them were still in the S or G2/M phase; however, some of them had moved to G0/G1. It was suggested that mitotic entry was inhibited at 4 and 8 HAT. At 12 HAT, the cells moved to G0/G1 or to the sub-G1 phase, which contained apoptotic cells. These

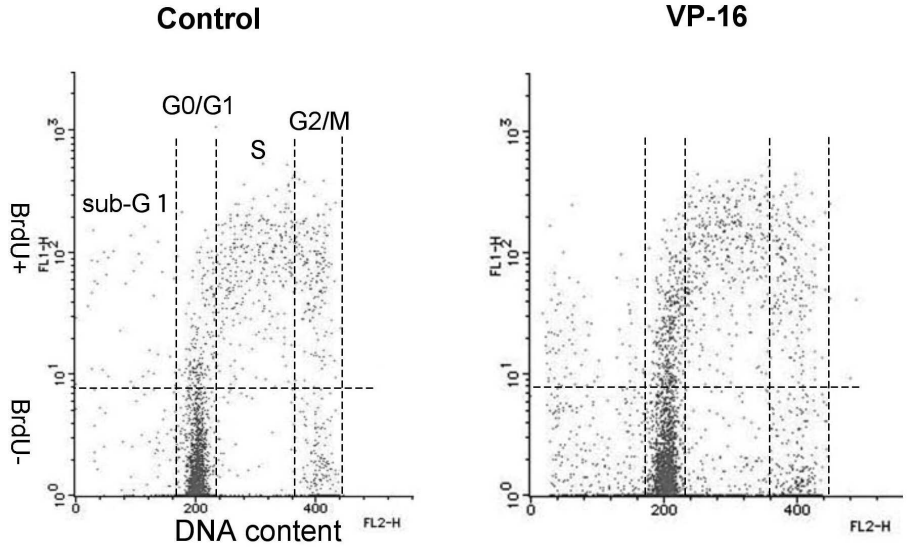

	Control	VP-16	
BrdU+ cells	11.8 ± 0.18 (%)	14.4 ± 2.81	
Sub-G1	2.4 ± 0.54	6.9 ± 0.38	**
G0/G1	86.2 ± 0.73	73.0 ± 2.85	
S	7.2 ± 0.92	11.3 ± 1.51	*
G2/M	4.7 ± 1.62	9.3 ± 2.16	*

Fig. 1. The BrdU-incorporating potency of telencephon cells in the VP-16-exposed fetuses remained unchanged as compared to the control fetuses at 4 HAT. S-phase accumulation was caused by the acceleration of G1/S transition rather than by the inhibition or arrest of DNA replication. The dams were injected with BrdU 1 hr before autopsy. The Horizontal and vertical axes denote the PI intensity (DNA content) and FITC intensity (BrdU incorporation), respectively. Cells with FITC intensity above the dotted line are BrdU-positive cells. The values represent the mean ± SD (n=3). *p<0.05, **p<0.01: significant difference from the control as revealed by Student's t test.

results indicate that cell cycle progression of the VP-16-exposed neural progenitor cells was blocked in G2 phase at 4 and 8 HAT, after which the cells either entered the G0/G1 phase or became apoptotic. Additionally, S-phase accumulation was shown at 4 and 8 HAT and some of the BrdU-positive S-phase cells directly underwent apoptosis at 4 HAT. The cell cycle progression of the neural progenitor cells was shown to be suppressed after VP-16 administration.

Western blot analysis (Fig. 3A) showed that VP-16 activates the ATM kinase pathway through auto-phosphorylation at serine 1981 from 2 to 8 HAT in the fetal telencephalons. Following ATM phosphorylation, γH2AX, an indicator of the induction of DNA DSBs, was observed from 4 to 12 HAT. The expression level of phospho-c-Abl protein (Try245), an indicator of proliferative activity, was decreased from 2 to 24 HAT. In the immunohistochemistry for γH2AX, the DNA DSBs marker, γH2AX, were shown in the S and G2-phase cells of the neural progenitor cells from 1 to 2 HAT after VP-16 exposure (Fig. 3B).

As shown in Fig. 4, the level of p53 increased from 2 to 8HAT after VP-16 administration. The level of p21, a Cdk inhibitor and the transcriptional gene of p53, increased from 4 to 12 HAT. The level of cyclin B1 increased from 2 to 8 HAT. The level of phospho-Cdc2 (Tyr15), an inactivated form of Cdc2, increased slightly from 2 to 8 HAT after VP-16 treatment. These results indicated that the VP-16-induced G2/M arrest was caused by p21, which inactivated the cyclin B-Cdc2 complex and eventually prevented mitotic entry. A decrease in the Cdc25A level was manifested from 2 to 24 HAT as a result of VP-16 exposure, indicating that Cdc25A might be phosphorylated by the checkpoint kinase 1 (Chk1) or Chk2 pathways, followed by its degradation, and finally it continues to inactivate Cdk2, which causes the inhibition of S-phase progression, i.e., the so-called S-phase delay. From the increase in cyclin A by VP-16, it was presumed that cyclin A-Cdk2 complex might induce the acceleration of G1/S transition.

The level of phospho-p53 (Ser15 and 20) and puma-α was increased by VP-16 treatment in the fetal telencephalons (Fig 5). Caspase-3 was activated in the fetal brain after VP-16 administration (Nam et al., 2006a). This suggests that VP-16-induced apoptosis is mediated via mitochondrial pathways in fetal mouse brain.

In fetal C57BL/6 wild-type mice, VP-16 administration induced more severe histopathological changes as compared to those in the fetal ICR mice. Pyknotic cells in the telencephalon of the VP-16 treated

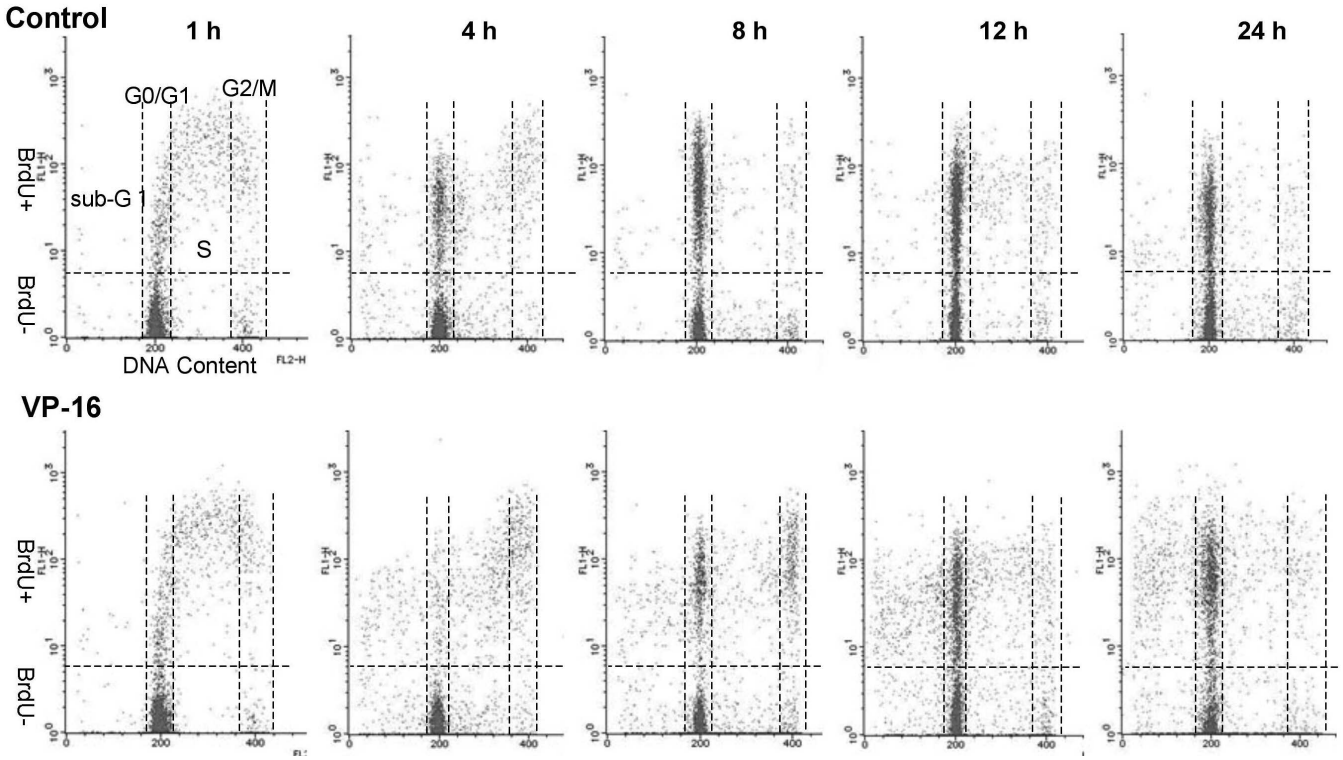

Fig. 2. Transition of the BrdU-incorporated telencephon cells of fetal mice in the cell cycle. Cell cycle progression of the VP-16-exposed cells was delayed as compared to the control cells. Most of the apoptotic cells incorporated BrdU. BrdU was injected with VP-16 or with a vehicle at the same time; (X axis: PI intensity (DNA content), Y axis: FITC intensity (BrdU incorporation)). Cells with FITC intensity above the dotted line are BrdU positive.

C57BL/6 mice were prominently observed in the CNS, including the brain and the spinal cord (Fig. 6). These results suggest that VP-16 caused more severe DNA damage or cell damage in the C57BL/6 rather than in the ICR mice. Pyknotic and TUNEL-positive cells of the VZ in the telencephalons were barely visible at 12 HAT in the fetal p53-/- mice. Apoptosis was almost abrogated in p53-deficient mice after VP-16 administration.

In the cell cycle analysis of p53-knockout mice (Fig. 7), the number of S-phase cells increased in every genotype at 4 HAT (+/+, 22.50±3.121%; +/-, 15.08±5.919%; -/-, 20.36±6.214%), while the number slightly increased only in the p53+/+ and p53+/- mice at 12 HAT (+/+, 17.55±5.104%; +/-, 13.81±5.332%; -/-, 11.09±6.380%). Thus, each *p53* genotype showed S-phase accumulation at 4 HAT, while only p53+/+ and p53+/- genotypes showed S-phase accumulation at at 12 HAT. The number of G2/M cells increased only in the p53+/+ and p53+/- mice at 4 HAT (+/+, 12.71±3.084%; +/-, 9.22±1.4631%; -/-, 6.77±1.193%). The number of apoptotic cells in the sub-G1 area also increased only in the p53+/+ and p53+/- mice (4 HAT; +/+, 6.95±2.578%; +/-, 2.58±1.047%; -/-, 0.77±0.250%, 12 HAT; +/+, 15.12±2.921%; +/-, 11.92±4.579%; -/-, 2.94±1.816%). In addition, p53-/- neural progenitor cells escaped from G2/M arrest and apoptosis at 4 HAT, although the number of cells in the S-phase increased through the 4 HAT. These results suggest that VP-16-induced G2/M arrest and apoptosis are p53-dependent phenomenon, but S-phase accumulation is a p53-independent phenomenon.

Discussion

In our previous study, an increase of the sub-G1 cells was observed in accordance with the sequential increase of the pyknotic and TUNEL-positive cells after VP-16 treatment. Moreover, S-phase accumulation and G2/M cell cycle arrest increased significantly at 4 HAT and 8 HAT. Based on these results, we conclude that VP-16 might induce S and G2/M arrest through its toxic effects and inhibit G2/M transition. The results of VP-16-induced cell cycle alternation were in concordance with the histopathological changes in the fetal brain occurring

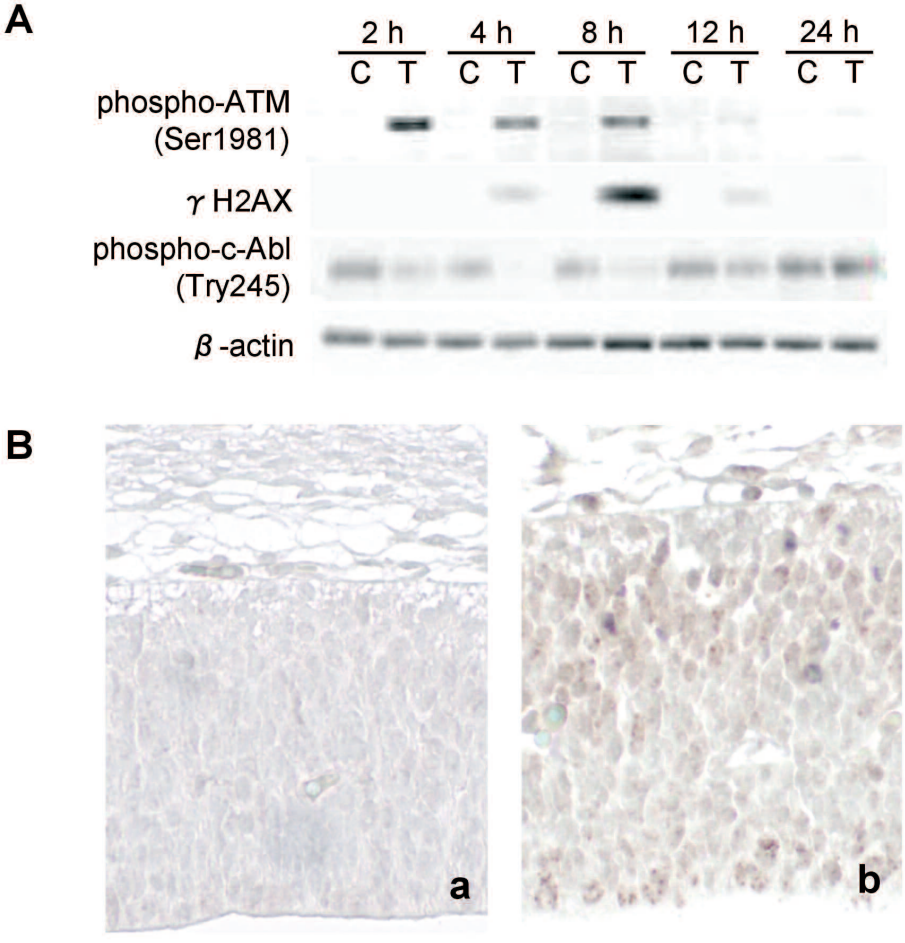

Fig. 3. VP-16 induced DNA damage, activation of ATM kinase through autophosphorylation, and a decrease in the proliferative activity of the neural progenitor cells. **A.** DNA damage and activation of ATM kinase after VP-16 treatment. Autophosphorylation of ATM at Ser1981, phosphorylation of H2AX at Ser139 and decrease in the phospho-c-Abl (Tyr245) level were confirmed. The total extracts from the control (C) and VP-16-treated (T) fetal telencephalons were analyzed by Western blot analysis. **B.** VP-16-induced DNA DSBs in the cells of the fetal mouse brain. Immunohistochemical examination the control **(a)** and VP-16-treated **(b)** fetal brain at 1 HAT for γH2AX; γH2AX foci were observed at 1 to 2 HAT after VP-16 administration. x 400

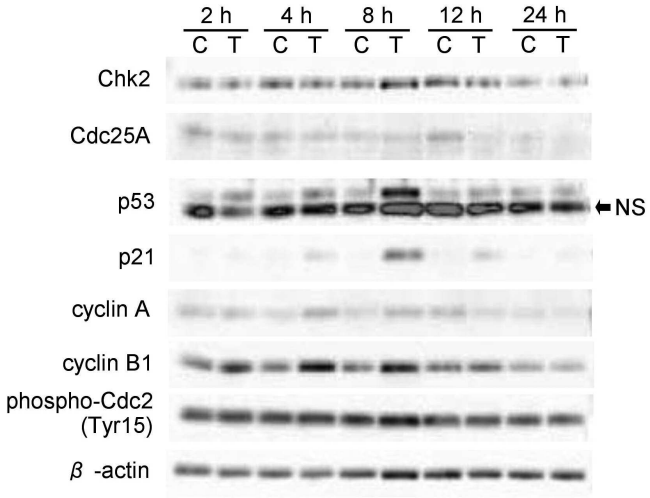

Fig. 4. Changes in the level of cell cycle control-related proteins in the fetal telencephalons. VP-16 increased the levels of p53, p21, cyclin A, cyclin B1 and phospho-Cdc2 (Tyr15) and decreased the Cdc25A level. The extracts from the control (C) and VP-16-treated (T) fetal telencephalons were analyzed by Western blot analysis.

as result of VP-16 administration.

S-phase accumulation in the VP-16-exposed telencephalons was caused by the acceleration of G1/S

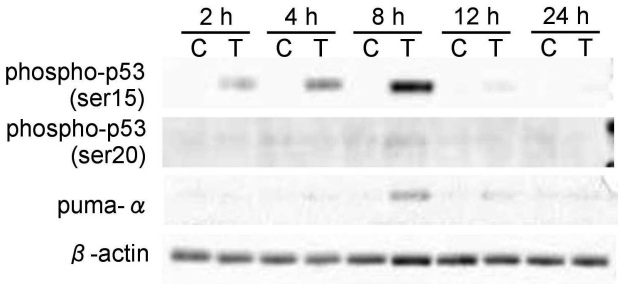

Fig. 5. Changes in the level of apoptosis-related proteins in the fetal telencephalons. VP-16 prominently increased the level of phospho-p53 (Ser15 and 20) and puma-·. The total level of proteins in the whole cell extracts was analyzed by Western blotting.

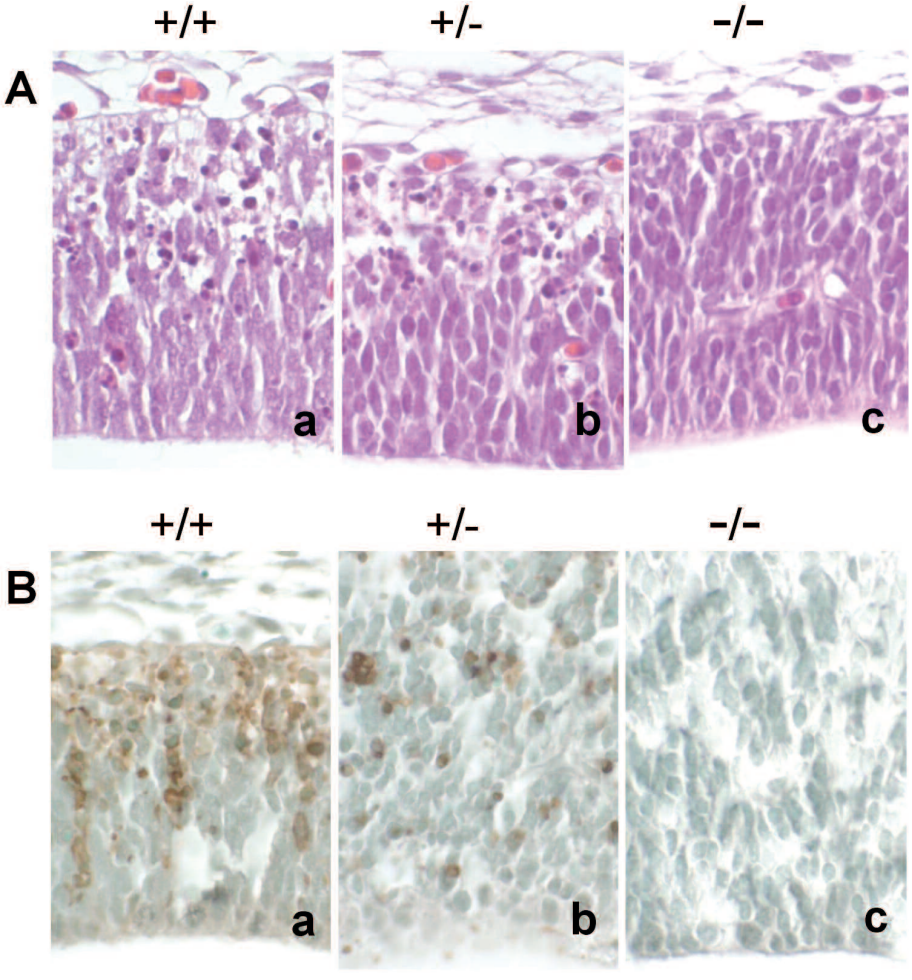

Fig. 6. A. Histological appearance of the telencephalons from p53+/+ (a), p53+/- **(b),** and p53-/- **(c)** fetuses at 12 HAT after VP-16-administration. VP-16-induced pyknotic cell death was almost completely abrogated in the p53-deficient fetuses. **B.** p53 is required for VP-16-induced apoptosis of neural progenitor cells. TUNEL staining of the telencephalons from p53+/+ **(a)**, p53+/- **(b)** and p53-/- **(c)** fetuses at 12 HAT after VP-16 treatment. VP-16-induced TUNEL-positive cells were not observed in the p53-deficient fetuses. x 400

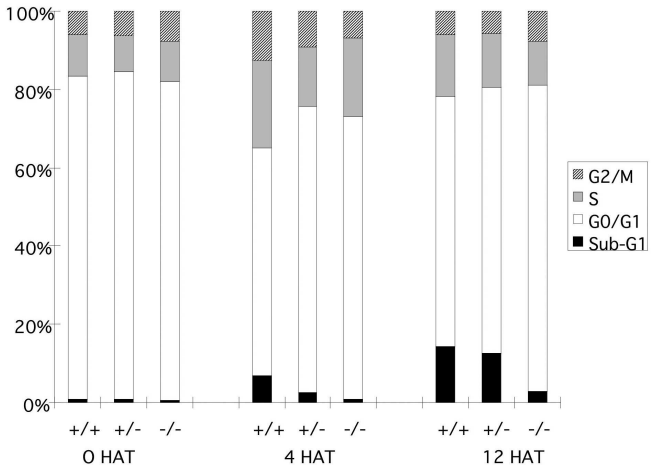

Fig. 7. Cell cycle alternation of the neural progenitor cells in the p53+/+, p53+/-, and p53-/- fetal mice by VP-16 treatment. The percentages for each cell cycle phase have been represented as the mean of all fetuses from the 5 dams. In p53+/+ and p53+/- mice, the number of S- and G2/M-phase cells increased at 4 HAT, and apoptosis in the sub-G1 area increased at 4 and 12 HAT. In p53-/- mice, the number of sub-G1 area and G2/M phase cells did not increase at 4 and 12 HAT, but the number of S-phase cells increased at 4 HAT.

transition rather than by the inhibition of S-phase progression (S-phase delay) at 4 HAT. From the decrease of phospho-c-Abl (Tyr245), however, it is presumed that the DNA proliferative activity of the neural progenitor cells in the telencephalons eventually decreased due to VP-16-induced cell damage and apoptosis. In pregnant mice concurrently injected with BrdU, the neural progenitor cell transition in the VP-16-exposed fetal telencephalons was delayed as compared to that in the control, and BrdU-positive signals were observed in many apoptotic cells from 4 to 24 HAT. This indicates that VP-16 damages proliferative neural progenitor cells, mainly the S-phase cells.

ATM kinase is involved in the regulation of cellular responses to irradiation and topoisomerase inhibitors (Samuel et al., 2002). DSBs are caused by irradiation and anti-tumor agents, by cleavage during recombination or collapse of replication forks. ATM is auto-phosphorylated since DSBs may occur as a part of the physiological process (Taylor, 1998). The ATM phosphorylate targets include p53, mdm2, Chk2, NBS1, and BRCA1. Although phospho-Chk 2 (Thr68) was not confirmed in this study, it was certain that the activated ATM phosphorylated Chk 2, which induced the phosphorylation of p53 at Ser15.

It is known that DNA damage-dependent focal accumulation of both DNA repair factors and γH2AX is observed in the nucleus, i.e., so-called repair foci. Histone H2AX phosphorylates at Ser128 (γH2AX) in the region of the nucleosome where DNA enters and exits in response to DNA damage, which induces DNA DSBs. In the absence or mutation of H2AX, the NHEJ and HR pathways are impaired or fail, suggesting that H2AX phosphorylation has an important role in the initiation of DNA repair (Downs et al., 2000).

In response to genotoxic stress such as ultraviolet light or ionizing radiation, Chk1 and Chk2 phosphorylate Cdc25A at Ser123. The phosphorylation of Cdc25A at serine 123 is a signal for ubiquitination and subsequent degradation of Cdc25A. The decrease in Cdc25A is continued, thereby inactivating Cdk2, which in turn, inhibits cell replication (S-phase delay) (Mailand et al., 2001; Bartek et al., 2004). Overexpression of cyclin A accelerates the entry of mammalian cells into the S-phase, indicating that cyclin A could be a limiting factor that is required for triggerring replication (Resnitzky et al., 1995). The cyclin A-Cdk2 complex is known to activate DNA synthesis through the replication complex and to inhibit the assembly of new complexes (Coverley et al., 2002).

Maintenance of G2 arrest is known to be assured by p21-dependent inactivation of mitotic Cdks (cyclin B1-Cdc2 and cyclin A-Cdc2). Cyclin B1-Cdc2 complexes are maintained in an inactive state by association with p21, which provokes nuclear retention of cyclin B1-Cdc2 and prevents their activation at the centrosome and, possibly, in the cytoplasm and nucleus (Charrier-Savournin et al., 2004). p21 binds with the cyclin B-Cdc2 complex and blocks the activated phosphorylation of Cdc2 on Thr161 by Cdk-activation kinase (Smits et al., 2000). Further, VP-16 has been shown to induce p21 up-regulation in a p53-dependent manner via ATM/ATR pathway in an in vitro experiment (Ding et al., 2003). Cyclin A1 has been shown to be up-regulated in VP-16-treated tumor cells undergoing p53-dependent apoptosis (Rivera et al., 2006).

In the fetal brain of p53-knockout mice, VP-16-induced S-phase accumulation occurred, but G2/M arrest and apoptosis were not observed. It has been shown that p53 is necessary for VP-16-induced G2/M arrest and apoptosis, but not crucial for VP-16-induced S-phase accumulation. However, S-phase accumulation in the p53+/+ and p53+/- fetal mice at 12 HAT resulted from an increase in the number in early S-phase cells. An increase in cyclin A following G2/M arrest at 4 and 12 HAT may presumably enhance G1/S transition at 12 HAT in the p53+/+ and p53+/- fetal mice. Following the activation of the p53 pathway by VP-16 treatment, up-regulation of p21 was blocked in the G2 phase, which eventually increased cyclin A. On the other hand, p53 is not necessary for S-phase delay (inhibition of DNA replication) after VP-16 treatment. A decrease in Cdc25A after VP-16 treatment inhibited Cdks and finally blocked S-phase progression via the activation of an ATM-related and p53-independent pathway.

VP-16 causes DNA damage in neural progenitor cells in the S and G2 phases, induces S-phase accumulation and G2/M arrest, and evokes apoptosis. VP-16-induced DNA damage occurs through ATM-kinase activation. ATM autophosphorylation might be

required for VP-16-induced cell cycle alternation and apoptosis. Further investigation on DNA repair in neural progenitor cells after VP-16-induced DNA damage is necessary.

Acknowledgements. We are grateful to Dr. Akemi Koshiyama and Kazuyuki Mekada of RIKEN BioResource Center (Tsukuba, Japan), for providing the p53-knockout mice.

References

Bartek J., Lukas C. and Lukas J. (2004). Checking on DNA damage in S phase. Nat. Rev. Mol. Cell Biol. 20045, 792-804.

Charrier-Savournin F.B., Chateau M.T., Gire V., Sedivy J., Piette J. and Dulic V. (2004). p21-mediated nuclear retention of cyclin B1-Cdk1 in response to genotoxic stress. Mol. Biol. Cell. 15, 3965-3976.

Chen A.Y. and Liu L.F. (1994). DNA topoisomerases: essential enzymes and lethal targets. Annu. Rev. Pharmacol. Toxicol. 34, 191-218.

Coverley D., Laman H. and Laskey R.A. (2002). Distinct roles for cyclins E and A during DNA replication complex assembly and activation. Nat. Cell Biol. 4, 523–528.

Ding H., Duan W., Zhu W.G., Ju R., Srinivasan K., Otterson G.A. and Villalona-Calero M.A. (2003). p21 respense to DNA damage induced by genistein and etoposide in human lung cancer cells. Biochem. Biophys. Res. Commun. 305, 950-956.

DiTullio R.A., Mochan T.A., Venere M., Bartkova J., Sehested M., Bartek J. and Halazonetis T.D. (2002). 53BP1 functions in an ATM-dependent checkpoint pathway that is constitutively activated in human cancer. Nat. Cell Biol. 4, 998-1002.

Downs J.A., Lowndes N.F. and Jackson S.P. (2000). A role for Saccharomyces cerevisiae histone H2A in DNA repair. Nature 408, 1001-1004.

D'Sa-Eipper C., Leonard J.R., Putcha G., Zheng T.S., Flavell R.A., Rakic P., Kuida K. and Roth K.A. (2001). DNA damage-induced neural precursor cell apoptosis requires p53 and caspase 9 but neither Bax nor caspase 3. Development 128, 137-146.

Fujita S. (2003) The discovery of the matrix cell, the identification of the multipotent neural stem cell and the development of the central nervous system. Cell Struct. Funct. 28, 205-228.

Gantchev T.G. and Hunting D.J. (1997). Enhancement of etoposide (VP-16) cytotoxicity by enzymatic and photodynamically induced oxidative stress. Anticancer Drugs 8, 164-173.

Ha L., Ceryak S. and Patierno S.R. (2003). Chromium (VI) activates ataxia telangiectasia mutated (ATM) protein. Requirement of ATM for both apoptosis and recovery from terminal growth arrest. J. Biol. Chem. 278, 17885-17894.

Hande K.R. (1998). Etoposide: four decades of development of topoisomerase inhibitor. Eur. J. Cancer 34, 1514-1521.

Katayama K., Ueno M., Yamauchi H., Nagata T., Nakayama H. and Doi K. (2005) Ethylnitrosourea induces neural progenitor cell apoptosis after S-phase accumulation in a p53-dependent manner. Neurobiol. Dis. 18, 218-225.

Ko L.J. and Prives C. (1996) p53: puzzle and paradigm, Genes Dev. 10, 1054-1072.

Levine A.J. (1997). p53, the cellular gatekeeper for growth and division. Cell 88, 323-331.

Mailand N., Syljuasen R.G. and Lukas J. (2001). The ATM-Chk2-Cdc25A checkpoint pathway guards against radioresistant DNA synthesis. Nature 410, 842-8 47.

Nam C., Woo G.H., Uetsuka K., Nakayama H. and Doi K. (2006a). Histopathological changes in the brain of mouse fetuses by etoposide-administration. Histol. Histopathol. 21, 257-263.

Nam C., Yamauchi H., Nakayama H. and Doi K. (2006b). Etoposide induces apoptosis and cell cycle arrest of neuroepithelial cells in a p53-related manner. Neurotoxicol. Teratol. 28, 664-672.

Qian X., Shen Q., Goderie S.K., He W., Capela A., Davis A.A. and Temple S. (2000). Timing of CNS cell generation: a programmed sequence of neuron and glial cell production from isolated murine cortical stem cells. Neuron 28, 69-80.

Resnitzky D., Hengst L. and Reed S.I. (1995). Cyclin A-associated kinase activity is rate limiting for entrance into S phase and is negatively regulated in G1 by p27Kip1. Mol. Cell. Biol. 15, 4347–4352.

Rivera A., Mavila A., Bayless K.J., Davis G.E. and Maxwell S.A. (2006). Cyclin A1 is a p53-induced gene that mediates apoptosis, G2/M arrest, and mitotic catastrophe in renal, ovarian, and lung carcinoma cells. Cell. Mol. Life Sci. 63, 1425-1439.

Robinson M.J. and Oscheroff N. (1991). Effects of antineoplastic drugs on the post-strand-passage DNA cleavage/religation equilibrium of topoisomerase II. Biochemistry 30, 1807-1813.

Samuel T., Weber H.O. and Funk J.O. (2002) Linking DNA damage to cell cycle checkpoints. Cell cycle 1, 162-168.

Sieber S.M., Whang-Peng J., Botkin C. and Knutsen T. (1978). Teratogenic and cytogenetic effects of some plant-derived antitumor agents (vincristine, colochicine, maytasine, VP-16-213 and VM-216) in mice. Teratology 18, 31-48.

Smits V.A., Klompmaker R., Vallenius T., Rijksen G., Makela T.P. and Madema R.H. (2000). p21 inhibits Thr161 phosphoryltation of Cdcw to enforce the G2 DNA damage checkpoint. J. Biol. Chem. 275, 30638-30648.

Stewart Z.A. and Pietenpol J.A. (2001) p53 signaling and cell cycle checkpoints. Chem. Res. Toxicol. 14, 243-263.

Taylor A.M. (1998). What has the cloning of the ATM gene told us about ataxia telangiectasia. Int. J. Radiat. Biol. 73, 365-371.

Tsukada T., Tomooka Y., Takai S., Ueda Y., Nishikawa S., Yagi T., Tokunaga T., Takeda N., Suda Y., Abe S., Matsuo I., Ikawa Y. and Aizawa S. (1993). Enhanced proliferative potential in culture of cells from p53-deficient mice. Oncogene 8, 3313-3322.

Ueno M., Katayama K., Yamauchi H, Nakayama H. and Doi K. (2006). Cell cycle and cell death regulation of neural progenitor cells in the 5-azacytidine (5AzC)-treated developing fetal brain. Exp. Neurol. 198, 154-166.

Yoshikawa K. (2000). Cell cycle regulators in neural stem cells and postmitotic neurons. Neurosci. Res. 37, 1-14.

Accepted November 11, 2009